



Impact of the solar wind dynamic pressure on the Region 2 field-aligned currents

S. Nakano,^{1,2} G. Ueno,^{1,2} S. Ohtani,³ and T. Higuchi^{1,2}

Received 11 August 2008; revised 16 November 2008; accepted 19 December 2008; published 24 February 2009.

[1] The relationship between the Region 2 field-aligned currents and the solar wind dynamic pressure is investigated using magnetic field data from Defense Meteorological Satellite Program-F13 (DMSP-F13). The generation of the Region 2 currents is associated with the direction of the magnetic pressure gradient in the magnetosphere, in relation to that of the thermal pressure gradient. Past spacecraft observations have suggested that the spatial distribution of the magnetic pressure in the magnetosphere varies with the solar wind dynamic pressure. Therefore, we can expect that the Region 2 currents would depend on the solar wind dynamic pressure. We compared the Region 2 field-aligned current intensity at the altitude of the ionosphere, as derived using magnetic field data from DMSP-F13, with the solar wind dynamic pressure derived from OMNI2 hourly data. It was confirmed that the Region 2 current intensity depends on the solar wind dynamic pressure during magnetic storms. During nonstorm times, however, the correlation between the Region 2 currents and the solar wind dynamic pressure is weak. The weak correlation during nonstorm times suggests that the plasma pressure in the ring current region is also essential for the effect of the solar wind dynamic pressure on the Region 2 currents.

Citation: Nakano, S., G. Ueno, S. Ohtani, and T. Higuchi (2009), Impact of the solar wind dynamic pressure on the Region 2 field-aligned currents, *J. Geophys. Res.*, 114, A02221, doi:10.1029/2008JA013674.

1. Introduction

[2] The Region 2 currents [e.g., *Iijima and Potemra*, 1976] are field-aligned currents basically driven by gradients of thermal and magnetic pressure in the inner magnetosphere. Assuming that the conditions for hydromagnetic equilibrium are approximately satisfied and that the plasma thermal pressure is isotropic, the Region 2 field-aligned current density flowing into the ionosphere, $J_{\parallel,i}$, is written as [e.g., *Boström*, 1975; *Caudal and Blanc*, 1988; *Haerendel*, 1990]

$$J_{\parallel,i} = \frac{B_I}{2} \int \frac{2\mu_0 \mathbf{B}}{B^4} \cdot \left[\nabla p \times \nabla \left(\frac{B^2}{2\mu_0} \right) \right] \frac{ds}{B} \quad (1)$$

where \mathbf{B} represents the magnetic field, B the magnetic field intensity, B_I the magnetic field intensity at the ionospheric footprint, p the thermal pressure, and μ_0 the permeability. This equation suggests that the Region 2 currents are generated only if the gradients of the thermal and magnetic pressure are neither parallel nor antiparallel to each other [e.g., *Sato and Iijima*, 1979].

[3] Around the source of the Region 2 currents in the inner magnetosphere, both the thermal and magnetic pressure gradient are directed almost earthward. However, if both the thermal and magnetic pressure were purely axisymmetric and the gradients of both were fully directed earthward, the thermal and magnetic pressure gradients would be parallel to each other, and the Region 2 field-aligned currents would not be generated. Thus, it would be reasonable to say that deviation from axisymmetry is essential in the generation of the Region 2 currents.

[4] The Earth's magnetosphere is clearly not axisymmetric. Since the magnetospheric magnetic field is compressed by the solar wind on the dayside and depressed by the tail current on the nightside, the magnetic pressure in the inner magnetosphere is higher on the dayside than on the nightside as already reported in many observational studies [e.g., *Sugiura and Poros*, 1973; *Iijima et al.*, 1990; *Le et al.*, 2004]. On the other hand, the thermal pressure is almost axisymmetric [*Lui and Hamilton*, 1992] or it tends to be higher on the nightside than on the dayside [*De Michelis et al.*, 1999]. Thus, while the magnetic pressure gradient deviates sunward, the thermal pressure gradient does not. This geometry between the magnetic pressure gradient vector and the thermal pressure gradient vector is in agreement with the sense of the Region 2 currents [*Lui et al.*, 1994]. Accordingly, the Region 2 current intensity would depend on the day-night asymmetry in the magnetospheric magnetic pressure and the thermal pressure [e.g., *Antonova and Ganushkina*, 1997].

¹Institute of Statistical Mathematics, Research Organization of Information and Systems, Tokyo, Japan.

²Japan Science and Technology Agency, Tokyo, Japan.

³Johns Hopkins University Applied Physics Laboratory, Laurel, Maryland, USA.

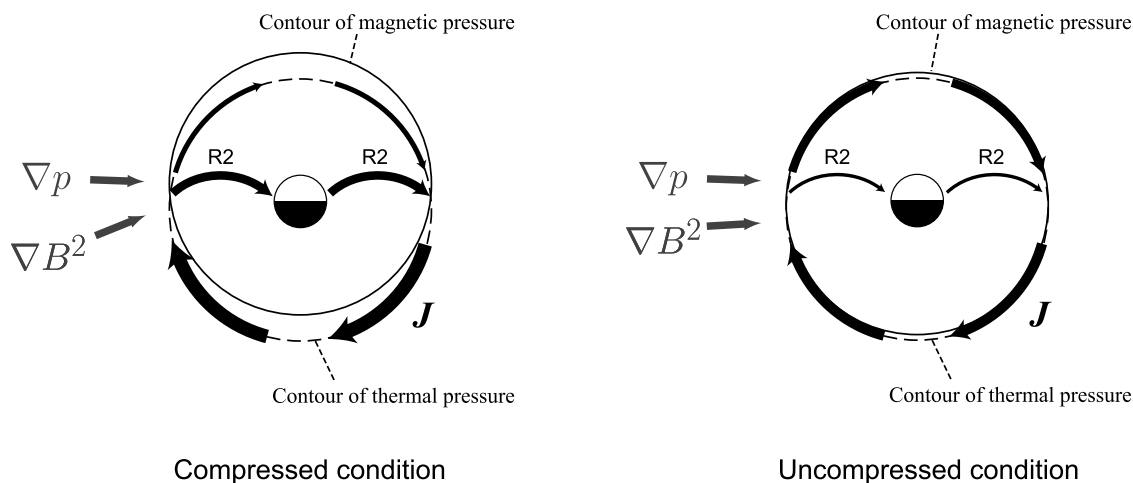


Figure 1. Graphical representation of the solar wind dynamic pressure effect on the Region 2 currents due to the deformation of the magnetospheric magnetic pressure distribution (see text for details).

[5] Space-based observations indicate that the day-night asymmetry in the magnetospheric magnetic pressure is strongly controlled by the solar wind dynamic pressure. *Tsyganenko et al.* [1999] demonstrated that the day-night asymmetry is accentuated under the influence of a high solar wind dynamic pressure. This indicates that the magnetospheric magnetic pressure distribution under the high solar wind dynamic pressure is favorable for the generation of the Region 2 currents. According to this argument, we can expect that the Region 2 currents may be controlled by the solar wind dynamic pressure as was also pointed out by *Mal'isev* [1997]. Figure 1 illustrates the effect of the solar wind dynamic pressure on the Region 2 currents due to the deformation of the magnetospheric magnetic pressure distribution. When the solar wind dynamic pressure is high (see Figure 1, left) and the front of the magnetosphere is compressed, the magnetic pressure in the inner magnetosphere shows a greater increase on the dayside than on the nightside. The direction of the magnetic pressure gradient would then deviate westward on the duskside, and eastward on the dawnside. The westward and eastward deviations drive field-aligned currents into and out of the ionosphere, respectively. Consequently, the Region 2 currents would be intensified when the solar wind dynamic pressure is enhanced. In contrast, when the solar wind dynamic pressure is low (see Figure 1, right), the day-night asymmetry in the magnetospheric magnetic pressure is smaller, and the generation of the Region 2 currents would become less efficient.

[6] The deformation of the magnetospheric magnetic pressure distribution due to the solar wind pressure enhancement could also affect the thermal pressure distribution, which is another factor associated with the generation of the Region 2 currents. For example, the enhancement of the dayside magnetic pressure could modify the drift trajectories of the ions and then the ion distribution in the inner magnetosphere. The thermal pressure gradient could then be modified accordingly. If temporal changes in the solar wind dynamic pressure occur abruptly, the thermal pressure distribution might be modified in another way. When the solar wind dynamic pressure rapidly increases, the magnetic field

strength in the inner magnetosphere also rapidly increases [e.g., *Kokubun*, 1983]. This rapid increase in the magnetic field strength would induce a rotational electric field ($\nabla \times \mathbf{E}$), which would accelerate ring current ions. This adiabatic acceleration process would also affect the thermal pressure distribution in the inner magnetosphere. Thus, the changes in the thermal pressure distribution could also contribute to the relationship between the solar wind dynamic pressure and the Region 2 currents.

[7] There have been a few observational studies which addressed the relationships between field-aligned currents and the solar wind dynamic pressure using magnetic field measurements from low-altitude satellites. *Iijima and Potemra* [1982] have investigated the relationships between the Region 1 currents and various solar wind parameters including the dynamic pressure. However, they did not examine the Region 2 currents. *Wang et al.* [2006] have suggested that the field-aligned current intensity depends on the solar wind dynamic pressure on the basis of an analysis of two geomagnetic storm events. However, they did not distinguish between the Region 1 currents and the Region 2 currents, and they did not examine statistical characteristics of the Region 2 currents. In order to confirm that the intensity of the Region 2 currents depends on the solar wind dynamic pressure, we statistically examine the relationship between the solar wind dynamic pressure and the intensity of the Region 2 field-aligned current, as derived from magnetic field measurements by the Defense Meteorological Satellite Program-F13 (DMSP-F13) satellite. We then discuss how the Region 2 currents are controlled by the solar wind dynamic pressure.

2. Analysis

2.1. Identification of the Region 2 Currents

[8] DMSP-F13 is a Sun-synchronous satellite on a nearly circular polar orbit at an altitude of around 840 km. It crosses the northern (southern) polar region from dusk to dawn (dawn to dusk). We used magnetic data obtained from March 1995 to July 2000, and selected the data on the dawnside from 0300 to 0900 magnetic local time (MLT) and those on the duskside from 1500 to 2100 MLT.

[9] A field-aligned current sheet was identified using an automatic technique developed by *Higuchi and Ohtani* [2000a, 2000b]. This technique uses the maximum-variance component of the magnetic field in the plane perpendicular to the background field to determine the orientation of large-scale field-aligned current sheets. The maximum-variance component along each orbit is fit by a first-order B spline function with variable node positions. A line segment between two adjoining nodes on the B spline function is regarded as a single current sheet (see *Higuchi and Ohtani* [2000b] for details).

[10] We selected the current sheet at the lowest latitude for each path across the auroral region. If the current sheet at the lowest latitude was directed upward/downward for a dawnside/duskside path, it was identified as a Region 2 current sheet. We excluded the current sheets for latitudes (altitude-adjusted corrected geomagnetic latitudes (AACGM)) of the center of the current sheet higher than 70° because we might misidentify the high-latitude Region 0 current sheet as the Region 2 current sheet when both the Region 1 and the Region 2 currents should vanish. We also excluded the current sheets for the cases that the solar zenith angle of their magnetic footprint is less than 90° to eliminate the dependence on the ionospheric conductivity indicated by some statistical studies [*Fujii and Iijima*, 1987; *Haraguchi et al.*, 2004; *Ohtani et al.*, 2005]. The number of the current sheets which we identified in the dark region was 1596 on the duskside and 1032 on the dawnside. We statistically compare the intensities of the current sheets in the dark region with the solar wind dynamic pressure which was derived from the OMNI2 hourly data. Since it has been suggested that the Region 2 currents exhibit a dawn-dusk asymmetry [e.g., *Anderson et al.*, 2005], the comparisons are conducted for the duskside current sheets and the dawnside current sheets separately.

[11] In our analysis, we refer to the D_{st} index as a proxy of the ring current intensity. As described above, the intensity of the Region 2 currents is dependent on the thermal pressure gradient as well as the magnetic pressure gradient. This thermal pressure gradient drives electric currents perpendicular to the magnetic field, which forms a main portion of the ring current. Thus, it is expected that the intensity of the Region 2 currents is related with the D_{st} index. However, the D_{st} index is affected not only by the ring current but also by the magnetopause current which highly depends on the solar wind dynamic pressure. The effect of the magnetopause current was then removed using the following equation provided by [*Burton et al.*, 1975]

$$D_{st}^* = D_{st} - b\sqrt{P_d} + c. \quad (2)$$

where P_d is the solar wind dynamic pressure. Here we set $b = 7.26 \text{ nT/nPa}^{1/2}$ and $c = 11 \text{ nT}$ according to *O'Brien and McPherron* [2000]. The D_{st} index also contains a contribution from the tail current as well as a contribution from the ring current [e.g., *Turner et al.*, 2000; *Ohtani et al.*, 2001; *Ganushkina et al.*, 2004; *Kalegaev et al.*, 2005]. However, even if the tail current contribution is significant, at least the main part of D_{st}^* variations would be due to the ring current contribution. Hence, it would be no problem to assume that the ring current is developed when the absolute value of D_{st}^*

is larger and that the ring current is weak when the absolute value of D_{st}^* is small. Then, we classified all the observations into three categories: non-storm-time observations ($-20 \leq D_{st}^* < 10$), weak-storm-time observations ($-50 \leq D_{st}^* < -20$), and moderate-storm-time observations ($-80 \leq D_{st}^* < -50$). Observations with $D_{st}^* < -80$ or $D_{st}^* \geq 10$ were not used, because sufficient data are not available.

2.2. Elimination of the Convection Effect

[12] It should be noted that the intensity of the Region 2 currents is closely associated with the magnetospheric and ionospheric convection because the electric field due to the global convection maintains the azimuthal thermal pressure gradient in the inner magnetosphere [e.g., *Vasyliunas*, 1970; *Jaggi and Wolf*, 1973; *Caudal and Blanc*, 1988]. Since the enhancement of the solar wind dynamic pressure could affect the magnetospheric and ionospheric convection [*Boudouridis et al.*, 2005, 2007; *Kivelson and Ridley*, 2008], the Region 2 currents might correlate with the solar wind pressure via the magnetospheric and ionospheric convection. Even if the enhancement of the solar wind dynamic pressure did not affect the magnetospheric convection, the effects of the global convection could induce a spurious correlation between the intensity of the Region 2 currents and the solar wind dynamic pressure because the solar wind electric field would slightly correlate with the solar wind dynamic pressure.

[13] Since the contribution from the convection is not our present concern, we eliminate the effects of the magnetospheric and ionospheric convection. In order to eliminate the contribution from the convection, we refer to the PCN index [*Troshichev et al.*, 1988]. The PCN index is derived from the horizontal magnetic field at a single near-pole station (Thule) and it represents magnetic activity related to the magnetospheric and ionospheric convection. Figures 2 and 3 compare the intensity of the Region 2 currents on the duskside and that on the dawnside, respectively, with the PCN index. The top plot in Figures 2 and 3 is for non-storm-time observations ($-20 \leq D_{st}^* < 10$), the middle plot is for weak-storm-time observations ($-50 \leq D_{st}^* < -20$), and the bottom plot is for moderate-storm-time observations ($-80 \leq D_{st}^* < -50$). We then obtain a relationship between the Region 2 current intensity and the PCN index by fitting a linear regression model

$$J_{\parallel} = \alpha PCN + J_{\parallel 0} \quad (3)$$

to the current sheet data using the least squares method, where J_{\parallel} is the observed Region 2 current intensity. As the data are sparse and deviated from the linear model for $PCN \geq 3.5 \text{ mV/m}$, we exclude the data with $PCN \geq 3.5 \text{ mV/m}$ in this regression. The dashed line in each plot in Figures 2 and 3 shows the regression line for each D_{st}^* level. However, no significant D_{st}^* dependences are found in the relationship between the Region 2 current intensity and the PCN index. We then fit the linear models to the entire observations without classifications by D_{st}^* both for the duskside Region 2 data and for the dawnside Region 2 data. The solid line in each plot indicates the regression line using the entire observations. The values of the regression coefficients α and $J_{\parallel 0}$ in equation (3) were as follows: for the duskside, $\alpha = 0.0816 \pm 0.0030$, $J_{\parallel 0} = 0.0882 \pm 0.0040$; for the dawnside,

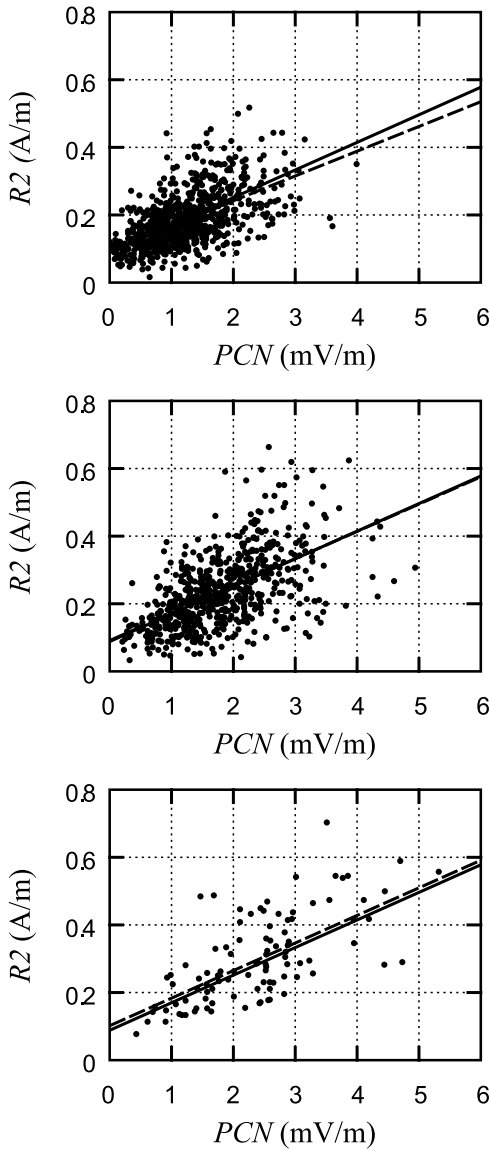


Figure 2. Comparisons between the intensity of the duskside Region 2 currents and the PCN index for (top) $-20 \leq D_{st}^* < 10$, (middle) $-50 \leq D_{st}^* < -20$, and (bottom) $-80 \leq D_{st}^* < -50$. The solid line in each plot indicates the regression line using the entire observations. The dashed line indicates the regression line for each D_{st}^* level.

$\alpha = 0.0737 \pm 0.0038$, $J_{\parallel 0} = 0.0913 \pm 0.0049$. Here the standard errors were estimated using the bootstrap method [Efron, 1981] with 10,000 resamplings. The standard errors obtained using the bootstrap method indicate uncertainties of statistics such as α and $J_{\parallel 0}$. The large uncertainties are mainly due to a lack of the data, and sometimes due to scatter of the data.

[14] We eliminate the dependences on the PCN index using the linear regression model in equation (3) as

$$J'_{\parallel} = J_{\parallel} - \alpha PCN. \quad (4)$$

Here J'_{\parallel} denotes the current intensity after eliminating the dependences on the PCN index. The data with $PCN \geq 3.5$ mV/m are hereafter excluded from the analysis because

the relationship between the Region 2 current intensity and PCN is deviated from the linear model as mentioned above. We then compare the values of J'_{\parallel} with the solar wind dynamic pressure.

3. Result

[15] Figure 4 compares the duskside Region 2 currents after eliminating the PCN dependence and the solar wind dynamic pressure; the top plot is for non-storm-time observations ($-20 \leq D_{st}^* < 10$), the middle plot is for weak-storm-time observations ($-50 \leq D_{st}^* < -20$), and the bottom plot is for moderate-storm-time observations ($-80 \leq D_{st}^* < -50$). During non-storm times, there is no clear correlation between the intensity of the duskside Region 2 currents and the solar wind dynamic pressure. However, during weak storms, the Region 2 current intensity shows a weak dependence on the solar wind dynamic pressure. The dependence

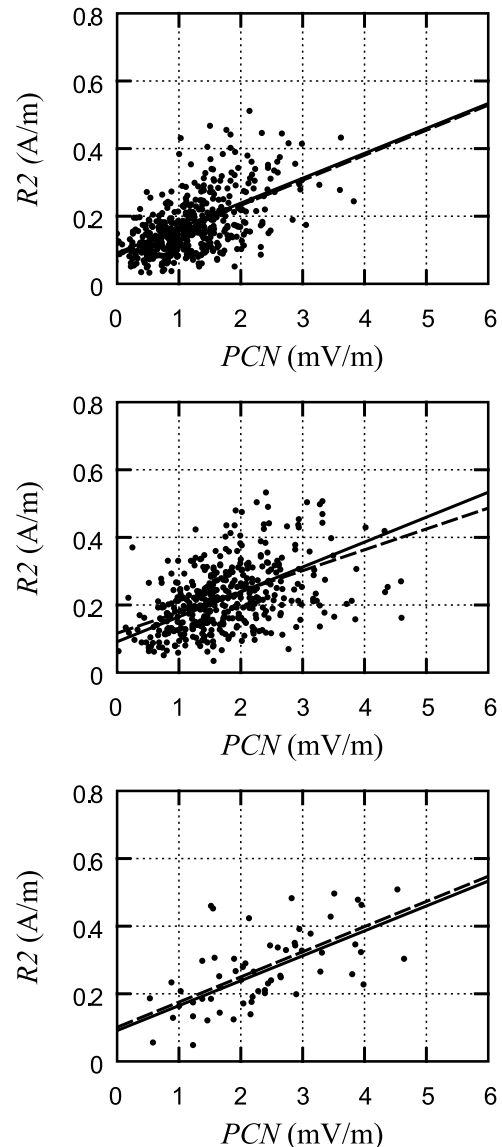


Figure 3. Same as Figure 2, but for the dawnside Region 2 currents.

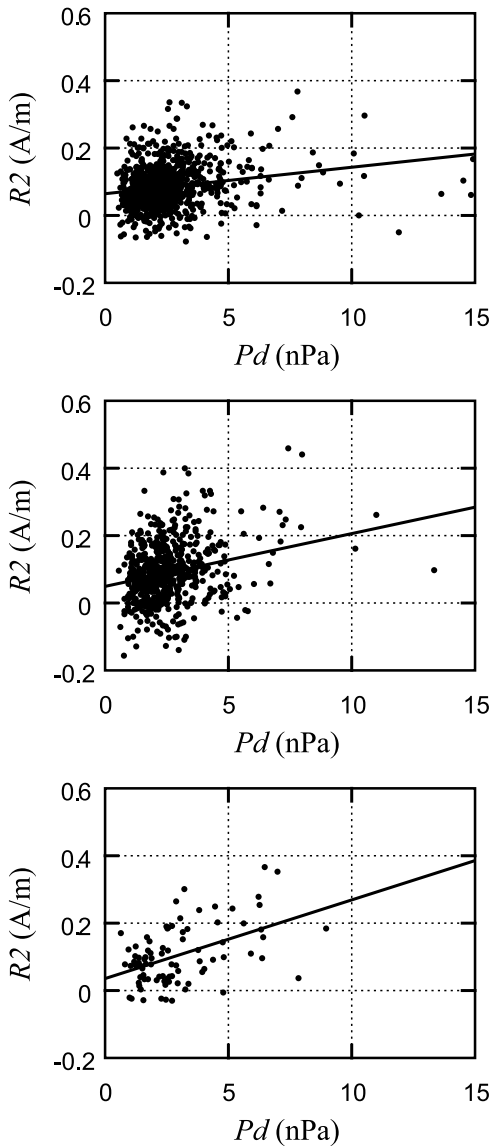


Figure 4. Comparisons of the intensity of the duskside Region 2 currents after eliminating the PCN dependence with the solar wind dynamic pressure (P_d) for (top) $-20 \leq D_{st}^* < 10$, (middle) $-50 \leq D_{st}^* < -20$, and (bottom) $-80 \leq D_{st}^* < -50$. The solid line in each plot indicates the regression line for each D_{st}^* level.

of the Region 2 current intensity on the solar wind dynamic pressure becomes clearer during moderate storms.

[16] We fit a linear regression model

$$J_{\parallel}^i = \beta P_d + J_{\parallel 0}^i \quad (5)$$

to the data for three different storm level categories using the least squares method. The estimated regression

Table 1. Estimated Regression Coefficients of a Linear Regression Model $J_{\parallel}^i = \beta P_d + J_{\parallel 0}^i$ for the Duskside Region 2 Currents

	β	$J_{\parallel 0}^i$
$-20 \leq D_{st}^* < 10$	0.0079 ± 0.0022	0.224 ± 0.006
$-50 \leq D_{st}^* < -20$	0.0157 ± 0.0038	0.209 ± 0.009
$-80 \leq D_{st}^* < -50$	0.0233 ± 0.0062	0.195 ± 0.017

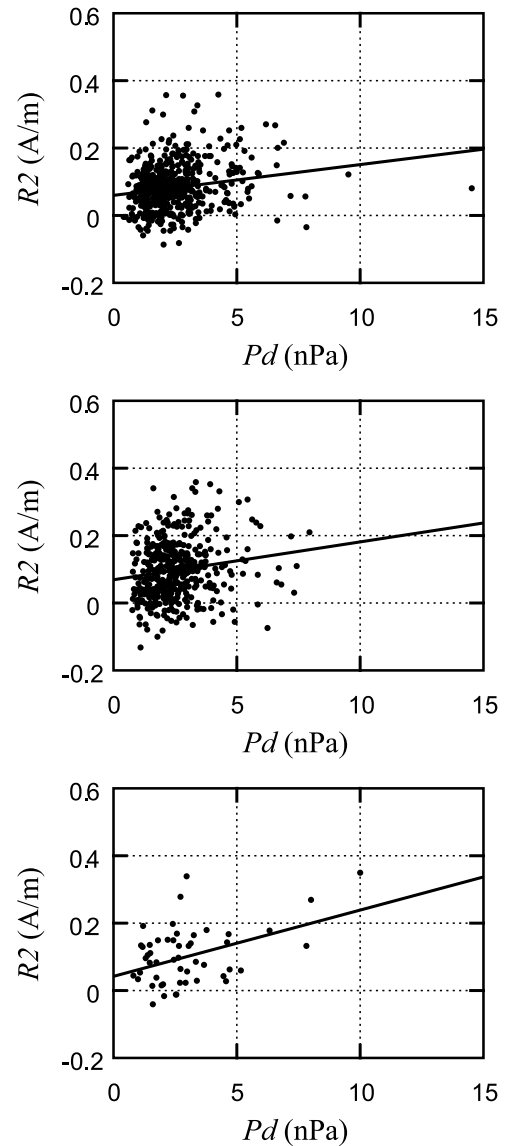


Figure 5. Same as Figure 4, but for the dawnside Region 2 currents.

coefficients are shown in Table 1, where the standard errors were estimated using the bootstrap method with 10,000 resamplings. The positive slopes of the regression lines for all three storm levels indicate that the duskside Region 2 currents basically tend to increase with the enhancement of the solar wind dynamic pressure. The slope of the regression line becomes steeper with a decrease in D_{st}^* . This suggests that the effect of the solar wind dynamic pressure on the duskside Region 2 currents depends on the ring current intensity.

[17] Figure 5 shows the same comparisons as Figure 4 but for the dawnside Region 2 currents. We fit the same linear regression model as equation (5) to the data for each storm level. The estimated regression coefficients for the dawnside are shown in Table 2, where the standard errors were estimated using the bootstrap method with 10,000 resamplings as done in Table 1. The characteristics of the dawnside Region 2 currents are basically the same as the duskside Region 2 currents. The slopes of the regression

Table 2. Estimated Regression Coefficients of a Linear Regression Model $J'_{\parallel} = \beta P_d + J'_{\parallel 0}$ for the Dawnside Region 2 Currents

	β	$J'_{\parallel 0}$
$-20 \leq D_{st}^* < 10$	0.0091 ± 0.0029	0.204 ± 0.007
$-50 \leq D_{st}^* < -20$	0.0112 ± 0.0040	0.213 ± 0.010
$-80 \leq D_{st}^* < -50$	0.0197 ± 0.0065	0.187 ± 0.021

lines are positive for all the three storm level, which indicates that the dawnside Region 2 currents tend to increase with the enhancement of the solar wind dynamic pressure. As was also seen for the duskside case, the effect of the solar wind dynamic pressure is stronger for moderate-storm-time observations than for non-storm-time and weak-storm-time observations. In comparison with the duskside case, the slope of the regression is less steep in the dawnside case, although the difference between the duskside and the dawnside for each storm level is small. This result could be consistent with the result shown by *Anderson et al.* [2005] who indicated that the Region 2 currents are stronger on the duskside than on the dawnside.

4. Discussion

[18] The bottom plot in Figures 4 and 5 shows that the intensity of the Region 2 currents increases with the enhancement of the solar wind dynamic pressure as we expected in section 1 if the ring current is enhanced both on the duskside and on the dawnside. On the contrary, the solar wind dynamic pressure has little effect on the Region 2 current intensity if the absolute value of the D_{st} index is small ($-20 \leq D_{st} < 10$). This finding suggests that the link between the Region 2 currents and the solar wind dynamic pressure is dependent on the ring current intensity. The ring current dependence can be interpreted in terms of the mechanism depicted in Figure 1 as follows. As mentioned in section 2, the ring current intensity is associated with the earthward thermal pressure gradient in the inner magnetosphere. When the ring current is enhanced and a large amount of hot ring current ions are stored in the inner magnetosphere, the earthward thermal pressure gradient becomes strong. Under this condition, the day-night asymmetry in the magnetic pressure, which is driven by enhancement in the solar wind dynamic pressure, should effectively generate the Region 2 currents as indicated in equation (1). On the contrary, when the ring current is weak and hot ring current ions are lacking in the inner magnetosphere, even if the magnetic pressure is highly asymmetrical between the dayside and the nightside, the generation of the Region 2 currents can be inefficient because of the small thermal pressure gradient present in that case.

[19] However, since the deformation of the magnetospheric magnetic pressure distribution could affect the thermal pressure distribution, it is necessary to take into account the change in the thermal pressure. The thermal pressure distribution is influenced by the magnetic pressure distribution in two ways. First, the thermal pressure distribution can change because of the transitions of drift trajectories of ions. If the day-night asymmetry in the magnetospheric magnetic pressure is accentuated because of the enhancement of the solar wind dynamic pressure, the

trajectories of the ring current ions would be deflected. Some portion of high-energy ions would come to flow out of the magnetopause before they reach the dayside [Takahashi and Iyemori, 1989, 1990], which would reduce the dayside ion density and thus the dayside thermal pressure. The direction of the thermal pressure gradient would then deviate eastward on the duskside, and westward on the dawnside, which would enhance the Region 2 currents. Second, when the solar wind dynamic pressure abruptly increases, the consequent abrupt increase in the magnetic pressure would adiabatically accelerate the ring current ions, which would affect the thermal pressure and thus the Region 2 currents. Since the increase in the magnetic field strength is larger on the dayside than on the nightside [Kokubun, 1983], the thermal pressure enhancement due to the adiabatic acceleration would be more effective on the dayside than on the nightside. Thus, it appears that the effect of the adiabatic acceleration could reduce the Region 2 currents according to equation (1). However, it should be noted that equation (1) assumes isotropic thermal pressure. Since the adiabatic acceleration enhances mainly the perpendicular pressure but has little effect on the parallel pressure, it is necessary to take into account the anisotropy in the thermal pressure.

[20] In order to take into account the plasma anisotropy, we start with the equation derived by *Boström* [1975]. Since the convective term is negligible in the inner magnetosphere [Voigt, 1986], the electric current perpendicular to the magnetic field, \mathbf{J}_{\perp} , satisfies

$$\mathbf{J}_{\perp} \left[1 - \frac{\mu_0 (p_{\parallel} - p_{\perp})}{B^2} \right] = \frac{\mathbf{B}}{B^2} \times \left[\nabla p_{\perp} + (p_{\parallel} - p_{\perp}) \frac{\nabla B}{B} \right] \quad (6)$$

where p_{\perp} and p_{\parallel} indicate the perpendicular thermal pressure and the parallel thermal pressure, respectively. Since the magnetic pressure is much higher than the thermal pressure in the inner magnetosphere, we neglect the second term in the bracket on the left-hand side in equation (6) as

$$\mathbf{J}_{\perp} = \frac{\mathbf{B}}{B^2} \times \left[\nabla p_{\perp} + (p_{\parallel} - p_{\perp}) \frac{\nabla B}{B} \right]. \quad (7)$$

$$\begin{aligned} \nabla \cdot \mathbf{J}_{\perp} &= \left[\nabla p_{\perp} + (p_{\parallel} - p_{\perp}) \frac{\nabla B}{B} \right] \cdot \nabla \times \frac{\mathbf{B}}{B^2} \\ &+ \frac{\mathbf{B}}{B^3} \cdot \left[\nabla (p_{\parallel} - p_{\perp}) \times \nabla B \right]. \end{aligned} \quad (8)$$

Equation (8) can be reduced to:

$$\nabla \cdot \mathbf{J}_{\perp} = -\frac{\mu_0 \mathbf{B}}{B^4} \cdot \left[\nabla (p_{\perp} + p_{\parallel}) \times \nabla \left(\frac{B^2}{2\mu_0} \right) \right]. \quad (9)$$

Therefore, the field-aligned current density flowing into the ionosphere, $J_{\parallel, I}$, is written as

$$\begin{aligned} J_{\parallel, I} &= \frac{B_I}{2} \int \frac{\mu_0 \mathbf{B}}{B^4} \cdot \left[\nabla (p_{\perp} + p_{\parallel}) \times \nabla \left(\frac{B^2}{2\mu_0} \right) \right] \frac{ds}{B} \\ &= \frac{B_I}{2} \int \frac{\mathbf{B}}{B^3} \cdot \left[\nabla (p_{\perp} + p_{\parallel}) \times \nabla B \right] \frac{ds}{B}. \end{aligned} \quad (10)$$

The perpendicular pressure p_{\perp} can be written as

$$p_{\perp} = \frac{Nm\langle v_{\perp} \rangle^2}{2} = N\langle M \rangle B \quad (11)$$

where $\langle \rangle$ indicates the ensemble mean, N denotes the number density of ions, and $M = mv_{\perp}^2/2B$ denotes the magnetic moment which is an adiabatic invariant. When the solar wind dynamic pressure abruptly increases and ∇B deviates sunward, ∇p_{\perp} would accordingly deviate sunward. Thus, ∇B and ∇p_{\perp} might be still nearly parallel to each other even after the increase of the solar wind dynamic pressure. On the other hand, ∇p_{\parallel} would not show rapid responses to the changes in the magnetic pressure, although it could be modified gradually owing to the changes in drift trajectories. Hence, the Region 2 currents driven by ∇p_{\parallel} would be enhanced by an abrupt increase of the solar wind dynamic pressure. Consequently, the Region 2 currents would show a net increase as a result of the enhancement of the solar wind dynamic pressure, even though the adiabatic acceleration is more effective on the dayside than on the nightside.

[21] Abrupt changes in the solar wind dynamic pressure might also induce other transient processes in the magnetosphere [e.g., *Fujita et al.*, 2005; *Boudouridis et al.*, 2008]. If such transient processes influence the Region 2 currents, the Region 2 currents could exhibit some significant transient behavior. In the analyses conducted above, we did not distinguish between transient events and steady high-pressure events. Hence, it should be noted that the results of the analyses are contaminated by some transient effects other than the adiabatic ion acceleration effect. At present, it is difficult to distinguish between transient events and steady events. The amount of the currently available DMSP data is too small to resolve the time scale and other characteristics of the transient processes. The transient effects on Region 2 currents will be investigated in a future study after a sufficient amount of data becomes available.

5. Conclusion

[22] We have investigated the relationship between the Region 2 field-aligned current intensity and the solar wind dynamic pressure. We eliminated the dependence on the magnetospheric and ionospheric convection by referring to the PCN index. The comparison between the Region 2 current intensity after eliminating the dependence on the global convection and the solar wind dynamic pressure indicates that the Region 2 current intensity increases with the solar wind dynamic pressure during magnetic storms when the absolute value of D_{st}^* is large. The dependence on the solar wind pressure can be explained by the transition of the geometry between the magnetic pressure gradient vector and the thermal pressure gradient vector due to the solar wind dynamic pressure enhancement. Under the high solar wind dynamic pressure, the magnetic pressure in the inner magnetosphere shows a greater increase on the dayside than on the nightside and thus the magnetic pressure gradient deviates toward the dayside both on the duskside and on the dawnside. In addition, the change in the magnetic pressure would influence the thermal pressure distribution, which could also contribute to the enhancement of the Region 2

currents. It was also found that the effect of the solar wind dynamic pressure on the Region 2 currents depends on D_{st}^* ; that is, while the Region 2 currents depend on the solar wind dynamic pressure during magnetic storms, the dynamic pressure does not have a significant effect on the Region 2 currents during non-storm times. The dependence of the Region 2 currents on D_{st}^* can be reasonably attributed to the change in the earthward thermal pressure gradient in the inner magnetosphere. When the absolute value of D_{st}^* is large and the ring current is enhanced, the earthward thermal pressure gradient is strong and the generation of the Region 2 currents due to the day-night asymmetry in the magnetic pressure would be effective. On the contrary, when the ring current is weaker, the earthward thermal pressure gradient is also weaker and the generation of the Region 2 currents would become less efficient.

[23] **Acknowledgments.** This research was partially supported by the Japanese Ministry of Education, Science, Sports and Culture via a Grant-in-Aid for Young Scientists (B), 19740306, 2007–2009. The magnetic field data from the DMSP satellite were provided by G. Wilson and the Air Force Research Laboratory. The D_{st} index was provided by the World Data Center for Geomagnetism at Kyoto University. The OMNI2 solar wind data were obtained from the NSSDC OMNIWeb database.

[24] Wolfgang Baumjohann thanks Athanasios Boudouridis and another reviewer for their assistance in evaluating this paper.

References

- Anderson, B. J., S.-I. Ohtani, H. Korth, and A. Ukhorskiy (2005), Storm time dawn-dusk asymmetry of the large-scale Birkeland currents, *J. Geophys. Res.*, *110*, A12220, doi:10.1029/2005JA011246.
- Antonova, E. E., and N. Y. Ganushkina (1997), Azimuthal hot plasma pressure gradients and dawn-dusk electric field formation, *J. Atmos. Sol. Terr. Phys.*, *59*, 1343.
- Boström, R. (1975), Mechanisms for driving Birkeland currents, in *Physics of the Hot Plasma in the Magnetosphere*, edited by B. Hultquist, p. 341, Plenum, New York.
- Boudouridis, A., E. Zesta, L. R. Lyons, P. C. Anderson, and D. Lummerzheim (2005), Enhanced solar wind geoeffectiveness after a sudden increase in dynamic pressure during southward IMF orientation, *J. Geophys. Res.*, *110*, A05214, doi:10.1029/2004JA010704.
- Boudouridis, A., L. R. Lyons, E. Zesta, and J. M. Ruohoniemi (2007), Dayside reconnection enhancement resulting from a solar wind dynamic pressure increase, *J. Geophys. Res.*, *112*, A06201, doi:10.1029/2006JA012141.
- Boudouridis, A., E. Zesta, L. R. Lyons, P. C. Anderson, and A. J. Ridley (2008), Temporal evolution of the transpolar potential after a sharp enhancement in solar wind dynamic pressure, *Geophys. Res. Lett.*, *35*, L02101, doi:10.1029/2007GL031766.
- Burton, R. K., R. L. McPherron, and C. T. Russell (1975), An empirical relationship between interplanetary conditions and Dst , *J. Geophys. Res.*, *80*, 4204.
- Caudal, G., and M. Blanc (1988), Magnetospheric convection during quiet or moderately disturbed times, *Rev. Geophys.*, *26*, 809.
- De Michelis, P., I. A. Daglis, and G. Consolini (1999), An average image of proton plasma pressure and of current systems in the equatorial plane derived from AMPTE/CCE-CHEM measurements, *J. Geophys. Res.*, *104*, 28,615.
- Efron, B. (1981), Nonparametric estimates of standard error: The jackknife, the bootstrap and other methods, *Biometrika*, *68*, 589.
- Fujii, R., and T. Iijima (1987), Control of the ionospheric conductivities on large-scale Birkeland current intensities under geomagnetic quiet conditions, *J. Geophys. Res.*, *92*, 4505.
- Fujita, S., T. Tanaka, and T. Motoba (2005), A numerical simulation of the geomagnetic sudden commencement: 3. A sudden commencement in the magnetosphere-ionosphere compound system, *J. Geophys. Res.*, *110*, A11203, doi:10.1029/2005JA011055.
- Ganushkina, N. Y., T. I. Pulkkinen, M. V. Kubyshkina, H. J. Singer, and C. T. Russell (2004), Long-term evolution of magnetospheric current systems during storms, *Ann. Geophys.*, *22*, 1317.
- Haerendel, G. (1990), Field-aligned currents in the Earth's magnetosphere, in *Physics of Magnetic Flux Ropes*, *Geophys. Monogr. Ser.*, vol. 58, edited by C. T. Russell, E. R. Priest, and L. C. Lee, p. 539, AGU, Washington, D. C.

- Haraguchi, K., H. Kawano, K. Yumoto, S. Ohtani, T. Higuchi, and G. Ueno (2004), Ionospheric conductivity dependence of dayside region-0, 1, and 2 field-aligned current systems: Statistical study with DMSP-F7, *Ann. Geophys.*, *22*, 2775.
- Higuchi, T., and S. Ohtani (2000a), Automatic identification of large-scale field-aligned current structures and its application to night-side current system, in *Magnetospheric Current Systems*, *Geophys. Monogr. Ser.*, vol. 118, edited by S. Ohtani et al., p. 389, AGU, Washington, D. C.
- Higuchi, T., and S. Ohtani (2000b), Automatic identification of large-scale field-aligned current structures, *J. Geophys. Res.*, *105*, 25,305.
- Iijima, T., and T. A. Potemra (1976), The amplitude distribution of field-aligned currents at northern high latitudes observed by Triad, *J. Geophys. Res.*, *81*, 2165.
- Iijima, T., and T. A. Potemra (1982), The relationship between interplanetary quantities and Birkeland current densities, *Geophys. Res. Lett.*, *9*, 442.
- Iijima, T., T. A. Potemra, and L. J. Zanetti (1990), Large-scale characteristics of magnetospheric equatorial currents, *J. Geophys. Res.*, *95*, 991.
- Jaggi, R. K., and R. A. Wolf (1973), Self-consistent calculation of the motion of a sheet of ions in the magnetosphere, *J. Geophys. Res.*, *78*, 2852.
- Kalegaev, V. V., N. Y. Ganushkina, T. I. Pulkkinen, M. V. Kubyshkina, H. J. Singer, and C. T. Russell (2005), Relation between the ring current and the tail current during magnetic storms, *Ann. Geophys.*, *23*, 523.
- Kivelson, M. G., and A. J. Ridley (2008), Saturation of the polar cap potential: Inference from Alfvén wing arguments, *J. Geophys. Res.*, *113*, A05214, doi:10.1029/2007JA012302.
- Kokubun, S. (1983), Characteristics of storm sudden commencement at geostationary orbit, *J. Geophys. Res.*, *88*, 10,025.
- Le, G., C. T. Russell, and K. Takahashi (2004), Morphology of the ring current derived from magnetic field observations, *Ann. Geophys.*, *24*, 1267.
- Lui, A. T. Y., and D. C. Hamilton (1992), Radial profiles of quiet time magnetospheric parameters, *J. Geophys. Res.*, *97*, 19,325.
- Lui, A. T. Y., H. E. Spence, and D. P. Stern (1994), Empirical modeling of the quiet time nightside magnetosphere, *J. Geophys. Res.*, *99*, 151.
- Mal'tsev, Y. P. (1997), Variations of field-aligned current caused by changes in solar-wind pressure, *Geomagn. Aeron.*, *37*, 125.
- O'Brien, T. P., and R. L. McPherron (2000), An empirical phase space analysis of ring current dynamics: Solar wind control of injection and decay, *J. Geophys. Res.*, *105*, 7707.
- Ohtani, S., M. Nosé, G. Rostoker, H. Singer, A. T. Y. Lui, and M. Nakamura (2001), Storm-substorm relationship: Contribution of the tail current to *Dst*, *J. Geophys. Res.*, *106*, 21,199.
- Ohtani, S., G. Ueno, and T. Higuchi (2005), Comparison of large-scale field-aligned currents under sunlit and dark ionospheric conditions, *J. Geophys. Res.*, *110*, A09230, doi:10.1029/2005JA011057.
- Sato, T., and T. Iijima (1979), Primary sources of large-scale Birkeland currents, *Space Sci. Rev.*, *24*, 347.
- Sugiura, M., and D. J. Poros (1973), A magnetospheric field model incorporating the OGO 3 and 5 magnetic field observations, *Planet. Space Sci.*, *21*, 1763.
- Takahashi, S., and T. Iyemori (1989), Three-dimensional tracing of charged particle trajectories in a realistic magnetospheric model, *J. Geophys. Res.*, *94*, 5505.
- Takahashi, S., and T. Iyemori (1990), Simulation of charged particle motions in realistic model magnetospheres and the effect of corotating electric field, *Ann. Geophys.*, *8*, 503.
- Troshichev, O., V. G. Andrezen, S. Vennerstrøm, and E. Friis-Christensen (1988), Magnetic activity in the polar cap—A new index, *Planet. Space Sci.*, *36*, 1095.
- Tsyganenko, N. A., G. Le, C. T. Russell, and T. Iyemori (1999), A study of the inner magnetosphere based on data of Polar, *J. Geophys. Res.*, *104*, 10,275.
- Turner, N. E., D. N. Baker, T. I. Pulkkinen, and R. L. McPherron (2000), Evaluation of the tail current contribution to *Dst*, *J. Geophys. Res.*, *105*, 5431.
- Vasyliunas, V. M. (1970), Mathematical models of magnetospheric convection and its coupling to the ionosphere, in *Particles and Fields in the Magnetosphere*, edited by B. M. McCormac, p. 60, D. Reidel, Dordrecht, Netherlands.
- Voigt, G.-H. (1986), Magnetospheric equilibrium configurations and slow adiabatic convection, in *Solar Wind-Magnetosphere Coupling*, edited by Y. Kamide and J. A. Slavin, p. 233, Terra Sci., Tokyo.
- Wang, H., H. Lühr, S. Y. Ma, J. Weygand, R. M. Skoug, and F. Yin (2006), Field-aligned currents observed by CHAMP during the intense 2003 geomagnetic storm events, *Ann. Geophys.*, *24*, 311.

T. Higuchi, S. Nakano, and G. Ueno, Institute of Statistical Mathematics, Research Organization of Information and Systems, Tokyo 106-8569, Japan. (higuchi@ism.ac.jp; shiny@ism.ac.jp; gen@ism.ac.jp)

S. Ohtani, Johns Hopkins University Applied Physics Laboratory, 11100 Johns Hopkins Road, Laurel, MD 20723-6099, USA. (Shin.Ohtani@jhuapl.edu)